

Original Article

Certain Analytical Aspects of Power Systems in the Presence of Facts Controllers - SVC and TCSC

Amita Mane^{1,2}, Shamik Chatterjee², Amol Kalage³

¹First Year Engineering Department, PCCOER, Pune, India

²School of Electronics and Electrical Engineering, Lovely Professional University, Phagwara, India

³Electrical Engineering Department, Sinhgad Institute of Technology, Lonavala, Pune, India

¹Corresponding Author : amita.mane@pccoer.in

Received: 25 April 2023

Revised: 17 June 2023

Accepted: 13 July 2023

Published: 21 July 2023

Abstract - Calculating power flows and voltages throughout a network under specific terminal or bus conditions is the power flow problem. The calculations of power flow are analyzed in power systems for planning, operational planning, the scheduling of economics and operation/control. Power flow equations, generally referred into power flow, are the key to power system operation. Effective power system performance with construction is generally done with the power flows. Newton-Raphson's (NR) method ensures that a good technique is applied for effectively tracking the power flow calculations. The effectiveness and the ability of the transmission lines to operate within critical parameters varies, mostly depending on the power system. So, to maintain a suitable voltage profile at multiple buses with changing power flow, the NR approach is applied. In this study, a MATLAB program to compute voltages, active, reactive power, and losses is developed in the selected systems, and to analyze the results for wide load variations, different transmission line parameters incorporated the compensators SVC and TCSC. The analysis is presented for the standard IEEE-14 bus system supporting graphical along with numerical results are presented.

Keywords - Power flow, Newton-Raphson's method, SVC, TCSC.

1. Introduction

Transmission lines in the power system are created to meet the demands of reactive and real power, as demanded by various connected loads in the network. The power flows are compulsory to analyze the steady-state solution to power systems at a given set of Bus-bar loads [1-3].

A computer model of how electricity flows through an interconnected system is known as a power-flow study or load-flow study in the field of power engineering. The power flows typically focus on various aspects of AC power parameters, such as voltages, voltage angles, real power, and reactive power, and typically use simplified notations like a one-line diagram and per-unit system. It examines power systems operating normally in a steady state [8-9].

1.1. Basic Requirements of Load Flow Studies

The basic requirements of load flows can be summed up as follows:

- The convergence properties
- The efficiency of computation and memory needs
- The convenience and flexibility of the implementation.

1.2. Requirements for Power Flows

Load flow studies are calculated for different conditions; points to consider are discussed below:

The line flows

- The bus voltage, along with the system voltage profile
- The effect of changes in configurations is incorporated with circuits in network loading
- The accompanying consequences of gearbox capability reductions and/or producing system loads
- The effect of in-phase and quadrature boost voltage on network loading effect
- Economic system operation
- System loss minimization
- Setting the transformer tap for economical operation
- Altering conductor diameters and system voltages may be able to improve an existing system.

1.3. Reviews of Load Flow Methods

The Gauss-Seidel iterative approach based on a nodal admittance matrix (also known as the admittance method below) was frequently employed in the early phases of employing digital computers to address power system load flow issues. This method's fundamentals are rather straightforward and only require a small amount of memory. These characteristics allowed it to fit the level of power system and computer theory at the time. Its convergence, nonetheless, is unsatisfactory. The number of iterations rises significantly as the system scale increases, and occasionally the iteration process is unable to converge.



Due to this issue, the sequential substitution approach, also known as the impedance method and based on the nodal impedance matrix, was used. [4].

In the early 1960s, the digital computer developed into the second generation. The memory and computing speed of computers were improved significantly, providing suitable conditions for the application of the impedance method. As mentioned above, the impedance matrix is a full matrix. The impedance method requires the computer to store the impedance matrix representing the power system's topology and parameters. Thus, it needs a great amount of computer memory. Furthermore, every element in the impedance matrix must be operated in each iteration, so the computing burden is very heavy.

The admittance approach was unable to resolve some load flow issues, while the impedance method was able to enhance convergence. Since then, the impedance approach has been widely used and has significantly impacted power system design, operation, and research.

The impedance method's primary drawbacks are its high memory requirements and computational overhead. The severity of these flaws increases with the size of the system. The piecewise solution approach based on the impedance matrix was created [17] to get over the drawback. Only the impedance matrices of local systems and the impedances of the lines between these local systems have to be recorded in the computer when using this approach to partition a big system into multiple tiny local systems. The need for memory and the workload associated with computation are considerably reduced in this way.

Applying the Newton-Raphson technique is another strategy to overcome the impedance method's limitations. Mathematicians frequently solve nonlinear equations using the Newton technique, which has a very favorable convergence [6-7]. The Newton method's computing efficiency may be significantly increased as long as the Jacobean matrix's scarcity is taken advantage of throughout the iterative phase. Since the middle of the 1960s, when the optimum order elimination approach first came into use, the Newton method has outperformed the impedance method in terms of convergence, memory requirement, and computation performance. Today, it is still the method of choice and is frequently employed for calculating load flows [11-13,19].

2. Modeling of Facts Controllers

2.1. Series Facts Controllers

Improve the capability of the current power systems by installing cutting-edge power electronics controllers, which are FACTS, often utilized nowadays. These FACTS controllers can work faster and more effectively to improve a

given system's performance. By adjusting system line impedance, these FACTS controllers may manage phase angle and voltage magnitudes at various system buses along active and reactive power flows on transmission lines.

2.1.1. Operating Principle of TCSC

Thyristor-controlled series controllers are the most often used variable impedance type FACTS controllers. The power flow in the transmission line to which it is attached is managed by this controller. Fig. 1 depicts the TCSC's basic structure. This fundamental design comprises a series reactor (TCR) operated by a thyristor and an antiparallel-linked capacitor. The power flows in transmission lines are managed by varying the net impedance of the lines using this device. When compared to other series controllers, this device's structure and function are the easiest to understand.

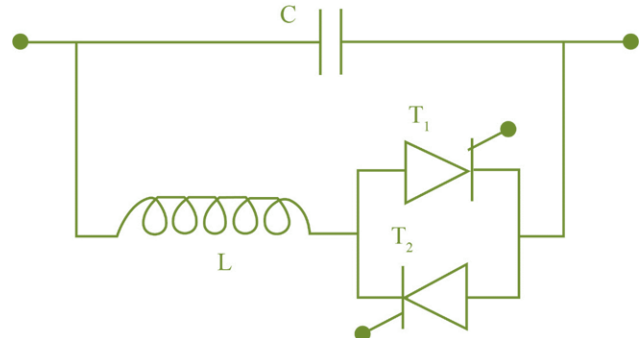


Fig. 1 Modelling of the TCSC

A system should include the examination of this device's impacts, according to TCSC. For this, the device's power injection model is explained as follows: Between bus-s and bus-r, -equivalent parameters were coupled in a straightforward gearbox arrangement. From bus-s to bus-r, the real and reactive power flows may be expressed as

$$P_{sr} = V_s^2 G_{sr} - V_s V_r [G_{sr} \cos(\delta_{sr}) + B_{sr} \sin(\delta_{sr})] \quad (1)$$

$$Q_{sr} = -V_s^2 (B_{sr} + B_{sh}) - V_s V_r [G_{sr} \sin(\delta_{sr}) - B_{sr} \cos(\delta_{sr})] \quad (2)$$

Where

$$\delta_{sr} = \delta_s - \delta_r = -\delta_{rs}$$

The real and reactive power flows from bus-r to bus-s is

$$P_{rs} = V_r^2 G_{sr} - V_s V_r [G_{sr} \cos(\delta_{sr}) - B_{sr} \sin(\delta_{sr})] \quad (3)$$

$$Q_{rs} = -V_r^2 (B_{sr} + B_{sh}) + V_s V_r [G_{sr} \sin(\delta_{sr}) + B_{sr} \cos(\delta_{sr})] \quad (4)$$

2.1.2. Operating Principle of TCSC

Thyristor-controlled series controllers are the most often used FACTS series controllers of the variable impedance kind. This controller regulates the flow of electricity via the transmission line to which it is attached. Fig. 1 depicts the straightforward structure of TCSC. Antiparallel linked

capacitor and a series reactor (TCR) operated by a thyristor make up this fundamental construction. Power flow in a transmission line may be regulated with this device by changing the net impedance of the transmission line. When compared to other series controllers, this device's architecture and function are the easiest to understand and operate.

TCSC needs to be integrated into a certain system in order to be seen how this device works. For this, the device's power injection model is explained as follows:

Between bus-s and bus-r, -equivalent parameters were coupled in a straightforward gearbox arrangement. It is possible to write the actual reactive power flows from bus-s to bus-r as

$$P_{sr} = V_s^2 G_{sr} - V_s V_r [G_{sr} \cos(\delta_{sr}) + B_{sr} \sin(\delta_{sr})] \tag{5}$$

$$Q_{sr} = -V_s^2 (B_{sr} + B_{sh}) - V_s V_r [G_{sr} \sin(\delta_{sr}) - B_{sr} \cos(\delta_{sr})] \tag{6}$$

Where $\delta_{sr} = \delta_s - \delta_r = -\delta_{rs}$

The real and reactive power flows from bus-r to bus-s is

$$P_{rs} = V_r^2 G_{sr} - V_s V_r [G_{sr} \cos(\delta_{sr}) - B_{sr} \sin(\delta_{sr})] \tag{7}$$

$$Q_{rs} = -V_r^2 (B_{sr} + B_{sh}) + V_s V_r [G_{sr} \sin(\delta_{sr}) + B_{sr} \cos(\delta_{sr})] \tag{8}$$

2.1.3. Power Injection Version of TCSC

Figure 2 shows π model of the transmission line with TCSC connected between bus-s and bus-r. Under the steady state condition, the TCSC can be represented as a static reactance $-jX_C$. For the power flow equations, the controllable reactance X_C has directly used as the control variable.

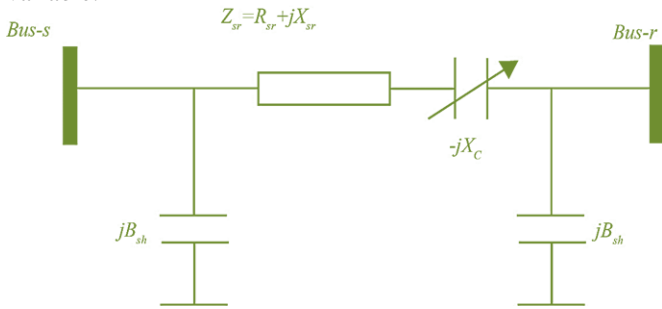


Fig. 2 Transmission line with TCSC

By connecting TCSC in series with the line, the line data will be altered. Following is a new line reactance formula

$$X_{srnew} = X_{sr} - X_C \tag{9}$$

Hence new line admittance between buses s and r can be derived as follows.

$$Y'_{sr} = \frac{1}{Z'_{sr}} = \frac{1}{R_{sr} + j(X_{sr} - X_C)}$$

$$Y'_{sr} = G'_{sr} + jB'_{sr} = \frac{R_{sr} - j(X_{sr} - X_C)}{R_{sr}^2 + (X_{sr} - X_C)^2}$$

$$G'_{sr} = \frac{R_{sr}}{R_{sr}^2 + (X_{sr} - X_C)^2} \tag{10}$$

$$B'_{sr} = -\frac{(X_{sr} - X_C)}{R_{sr}^2 + (X_{sr} - X_C)^2} \tag{11}$$

In line with series impedance and series reactance, renewed active and reactive power flows from bus-s to bus-r and from bus-r to bus-s, respectively.

$$P_{sr}^{TCSC} = V_s^2 G'_{sr} - V_s V_r (G'_{sr} \cos(\delta_{sr}) + B'_{sr} \sin(\delta_{sr})) \tag{12}$$

$$Q_{sr}^{TCSC} = -V_s^2 (B'_{sr} + B_{sh}) - V_s V_r (G'_{sr} \sin(\delta_{sr}) - B'_{sr} \cos(\delta_{sr}))$$

$$P_{rs}^{TCSC} = V_r^2 G'_{sr} - V_s V_r (G'_{sr} \cos(\delta_{sr}) - B'_{sr} \sin(\delta_{sr}))$$

$$Q_{rs}^{TCSC} = -V_r^2 (B'_{sr} + B_{sh}) + V_s V_r (G'_{sr} \sin(\delta_{sr}) + B'_{sr} \cos(\delta_{sr})) \tag{13}$$

The power loss in line with TCSC can be represented as:

$$P_{Loss} = P_{sr}^{TCSC} + P_{rs}^{TCSC} = G'_{sr} (V_s^2 + V_r^2) - 2V_s V_r G'_{sr} \cos(\delta_{sr})$$

$$Q_{Loss} = Q_{sr}^{TCSC} + Q_{rs}^{TCSC} = -(V_s^2 + V_r^2) (B'_{sr} + B_{sh}) + 2V_s V_r B'_{sr} \cos(\delta_{sr}) \tag{14}$$

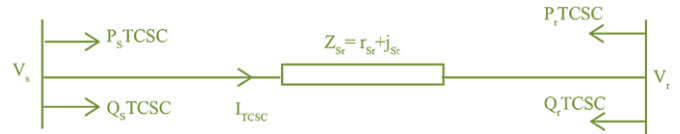


Fig. 3 Power injection model of TCSC

Because of TCSC, the alternate in-line float can be represented as a line without TCSC plus with power injected at the sending and receiving ends of the road with the tool, as shown in Fig.3. The active and reactive strength injections at bus-s and bus-r may be written as

Where,

$$P_s^{TCSC} = P_{sr} - P_{sr}^{TCSC} = V_s^2 \Delta G_{sr} - V_s V_r [\Delta G_{sr} \cos(\delta_{sr}) + \Delta B_{sr} \sin(\delta_{sr})] \tag{15}$$

$$P_r^{TCSC} = P_{rs} - P_{rs}^{TCSC} = V_s^2 \Delta G_{sr} - V_s V_r [\Delta G_{sr} \cos(\delta_{sr}) - \Delta B_{sr} \sin(\delta_{sr})] \tag{16}$$

$$Q_s^{TCSC} = Q_{sr} - Q_{sr}^{TCSC} = -V_s^2 \Delta B_{sr} - V_s V_r [\Delta G_{sr} \sin(\delta_{sr}) - \Delta B_{sr} \cos(\delta_{sr})] \tag{17}$$

$$Q_r^{TCSC} = Q_{rs} - Q_{rs}^{TCSC} = -V_r^2 \Delta B_{sr} + V_s V_r [\Delta G_{sr} \sin(\delta_{sr}) + \Delta B_{sr} \cos(\delta_{sr})] \tag{18}$$

TCSC tool is modeled with power injection version up to now by means of the use of the TCS Ss TCSC S r manipulate variable. Its miles are viable to calculate the complex power injected respectively.

$$S_s^{TCSC} = P_s^{TCSC} + jQ_s^{TCSC}, S_r^{TCSC} = P_r^{TCSC} + jQ_r^{TCSC}$$

Then, new power flow equations can be expressed by the following relationship.

$$\begin{bmatrix} \Delta P \\ \Delta Q \end{bmatrix} = \begin{bmatrix} H_{new} & M_{new} \\ N_{new} & L_{new} \end{bmatrix} \cdot \begin{bmatrix} \frac{\Delta \delta}{V} \\ \frac{\Delta V}{V} \end{bmatrix}$$

Where new mismatch vectors are

$$\Delta P_i = P_i^{spec} + P_i^{TCSC} - P_i^{Calc}; \forall i = s,r$$

$$\Delta Q_i = Q_i^{spec} + Q_i^{TCSC} - Q_i^{Calc}; \forall i = s,r$$

P_i^{spec} and Q_i^{spec} are the prescriptive real and reactive powers, P_i^{TCSC} and Q_i^{TCSC} are the power injection associated with TCSC devices, P_i^{calc} and Q_i^{calc} are computed using the power flow equations. Now, the mutated Jacobian matrix due to power injections of TCSC

$$H_{new} = H + \frac{\partial P_i^{TCSC}}{\partial \delta} \forall i = s,r; M_{new} = M + \frac{\partial P_i^{TCSC}}{\partial V} V \forall i = s,r$$

$$N_{new} = N + \frac{\partial Q_i^{TCSC}}{\partial \delta} \forall i = s,r; L_{new} = L + \frac{\partial Q_i^{TCSC}}{\partial V} V \forall i = s,r$$

H, M, N and L... These are the classic sub-Jacobian matrices.

2.2. Static Var Compensator(SVC)

Generator or absorber whose output is modified to alter the capacitive or inductive current to maintain or regulate particular electrical energy device (often bus Voltage) characteristics. To enhance device stability, SVCs are utilized in specific energy systems to embellish the voltage tiers. In use, the SVC can be thought of as an adjustable reactance with either reactance or firing-angle restrictions. The SVC nonlinear power equations are derived using the analogous circuit depicted in Fig. 4. Referring to Fig. 4, the SVC's current draw is

$$I_{SVC} = jB_{SVC}V_i. \tag{19}$$

Additionally, the SVC draws reactive power, which is likewise injected at bus-i, and this reactive power is

$$Q_{SVC} = Q_i = -V_i^2 B_{SVC}. \tag{20}$$

It is a 3-section static capacitor and/or inductors financial institution. When there is considerable loading, capacitor banks are required for excellent VAR and inductor banks are utilized for low VAR. As seen in Fig. 4, SVC is modelled in this thesis as an incredibly accurate reactive power injection at bus-i.

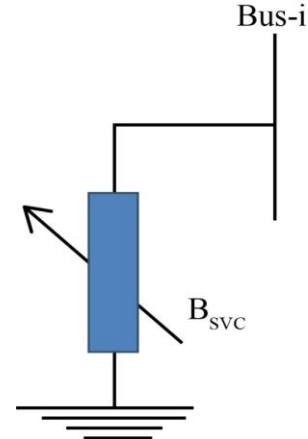


Fig. 4 Power injection model of SVC

3. Results and Analysis

The analytical aspects of the power system are performed on IEEE-14 bus systems [Ref]. It consists of 14 buses and 20 transmission lines, five generators located at buses 1,2,3,6 and 8; the remaining buses are the load buses and three tap changing transformers installed in lines 8 (4-7), 9 (4-9) and 10 (5-6).

There are total of four cases have been considered for the study of the two systems undertaken for analysis:

- Case 1: To perform load variations on the system from base values to 5% in steps of 1%.
- Case 2: To increase transmission parameters of the system from base values to 40% in steps of 10%.
- Case 3: To install SVC at the bus with minimum voltage.
- Case 4: To install TCSC in line with a maximum margin when compared to line limits.

3.1. Case-1

In case-1, to find out the impact of load fluctuation system performance, the load at each bus is varied from base values to 5% in steps of 1%. The NR load flow method tests the load variation and other system parameters' performance. Variation of voltage magnitude, variation of active power flow and variation of apparent power flow with increase in load for IEEE-14 bus system as shown in Table.1-3.

From the Table.1 it is set that the voltage magnitude at load buses has decreased as the load increases from the base value. Active power flow has increased in line 8, and reactive power flow has increased in line 14, consequently increasing active and reactive powers in line 15. The minimum voltage is obtained at bus-7 as a result of the redistribution of active power flow from the fourth bus and reactive power flow from the eighth bus towards bus-nine. The voltage magnitude at bus-7 is 1.6012 p.u. with 5% load, which is a 1% decrement when compared to the base case and the variations. The voltage magnitude is decreasing at all the buses on increasing the load from base value to 5% in steps of 1%.

Table 1. Variation in voltage magnitude with an increase in load for IEEE-14 Bus system

Bus No	Voltage Magnitude (p.u)					
	Base Case	1 % Load	2% Load	3% Load	4% Load	5% Load
1	1.06	1.06	1.06	1.06	1.06	1.06
2	1.045	1.045	1.045	1.045	1.045	1.045
3	1.01	1.01	1.01	1.01	1.01	1.01
4	1.022	1.0225	1.022	1.022	1.0218	1.0215
5	1.025	1.0250	1.024	1.0245	1.0243	1.0241
6	1.07	1.07	1.07	1.07	1.07	1.07
7	1.0626	1.0622	1.061	1.0617	1.0614	1.0612
8	1.09	1.09	1.09	1.09	1.09	1.09
9	1.0549	1.0545	1.054	1.0537	1.0533	1.0528
10	1.0500	1.0496	1.049	1.0488	1.0483	1.0479
11	1.0567	1.0560	1.055	1.0555	1.0553	1.0550
12	1.0551	1.055	1.054	1.0546	1.0545	1.0543
13	1.0501	1.0498	1.049	1.0493	1.0491	1.0498
14	1.0348	1.0342	1.033	1.0332	1.0326	1.0321

Similarly, the active power flow results are tabulated in the above Table.2. From this table; it is observed that the active power flow is increasing by increasing the load from base value to 5% steps of 1%. The active power flows from

bus-4 towards bus-9, which results in the decrease of voltage at bus-7 when the load is varied from base values to 5% in steps of 1%.

Table 2. Variation in active power flow with increase in load for IEEE-14 Bus system

Line No.	Active Power Flow (MW)					
	Base Case	1 % Load	2% Load	3% Load	4% Load	5% Load
1	86.241	88.174	90.109	92.048	93.989	95.934
2	48.240	49.075	49.911	50.748	51.585	52.423
3	40.494	41.230	41.966	42.704	43.442	44.181
4	41.401	41.937	42.747	43.011	43.548	44.086
5	31.362	31.748	32.134	32.520	32.906	33.293
6	-4.456	-4.687	-4.917	-5.148	-5.378	-5.608
7	-42.74	-43.36	-43.98	-44.60	-45.22	-45.84
8	18.423	18.693	18.963	19.233	19.503	19.7734
9	12.520	12.674	12.827	12.981	13.134	13.288
10	27.356	27.822	28.288	28.754	29.221	29.688
11	9.3545	9.4396	9.524	9.6102	9.6957	9.781
12	8.0300	8.1120	8.194	8.2762	8.3583	8.440
13	18.771	18.958	19.145	19.332	19.519	19.706
14	-10	-10	-10	-10	-10	-10
15	28.423	28.693	28.963	29.233	29.503	29.773
16	3.2604	3.302	3.344	3.386	3.429	3.471
17	8.1839	8.270	8.356	8.443	8.529	8.615
18	-5.749	-5.797	-5.845	-5.893	-5.941	-5.989
19	1.854	1.874	1.893	1.913	1.933	1.952
20	6.887	6.953	7.019	7.085	7.152	7.218

Variation in apparent power with an increase in load is shown in Table.3. It is observed that the apparent power flows

in the lines are increasing when the load is varied from base values to 5%.

Table 3. Variation in apparent power flow with increase in load for IEEE-14 Bus system

Line No.	Apparent Power Flow (MVA)						Line Limit
	Base Case	1 % Load	2% Load	3% Load	4% Load	5% Load	
1	86.274	88.222	90.175	92.134	94.097	96.066	150
2	48.432	49.263	50.094	50.927	51.760	52.592	85
3	41.245	41.946	42.649	43.354	44.061	44.771	85
4	41.417	41.953	42.489	43.026	43.563	44.100	85
5	31.367	31.753	32.139	32.526	32.913	33.300	85
6	8.796	8.714	8.643	8.584	8.537	8.501	85
7	43.387	44.023	44.660	45.296	45.932	46.568	150
8	20.099	20.340	20.582	20.824	21.067	21.311	30
9	12.531	12.686	12.841	12.996	13.151	13.307	32
10	30.691	31.071	31.455	31.841	32.229	32.620	45
11	9.810	9.920	10.030	10.141	10.253	10.365	14
12	8.377	8.466	8.554	8.643	8.731	8.820	32
13	20.009	20.222	20.434	20.647	20.860	21.074	22
14	19.290	19.423	19.556	19.690	19.824	19.960	32
15	29.445	29.746	30.047	30.348	30.650	30.951	29
16	5.884	5.896	5.909	5.992	5.935	5.949	32
17	9.137	9.215	9.294	9.373	9.452	9.531	18
18	5.824	5.883	5.942	6.003	6.064	6.126	12
19	1.959	1.982	2.005	2.028	2.052	2.075	12
20	7.008	7.083	7.159	7.234	7.310	7.387	12

3.2. Case-2

In case-2, to find out the effect of transmission parameters on system performance, the transmission parameters R and X in each line are varied from base values to 40% in steps of 10%. The variations in the system are as follows:

- The voltage magnitude in the system has decreased at all the lines when the R and X are increasing to 40% in steps of 10% due to an increase in reactive power in the line, as shown in Table.4.
- The transmission line's higher reactive power has led to an increase in losses. It is because transmission parameters have increased.
- The angle theta has increased due to the decrease in voltage in the system. It is due to an increase in transmission parameters.

From the above analysis, it is clear that the decrease in voltage, increase in losses and increase in angle is due to a major change in the reactive power flow in the transmission

line. The variations in voltage magnitude with the change in transmission parameters are shown in Table.4.

The table displays the changes in active power flow caused by changing gearbox characteristics. The table demonstrates that when the gearbox settings are increased to 40% in increments of 10%, the active power flow in the system is slightly rising.

The variations in apparent power flow with the change in transmission parameters are shown in Table.6. From Table.6; the apparent power flow is also increasing when the transmission parameters are increasing to 40% in steps of 10%.

In case 3, to analyze the effect of FACTs controllers on system performance, the basic variable impedance shunt (Static VAR Compensator-SVC) controller is considered by verifying the maximum load variation of the system.

Table 4. Variation in voltage magnitude with change in transmission parameter IEEE-14 Bus system

Bus No.	Voltage magnitude (p.u)					
	-10%	Base Case	10%	20%	30%	40%
1	1.060	1.060	1.060	1.060	1.060	1.060
2	1.045	1.045	1.045	1.045	1.045	1.045
3	1.012	1.000	1.010	1.010	1.010	1.010
4	1.025	1.023	1.021	1.020	1.018	1.016
5	1.027	1.025	1.024	1.023	1.021	1.020
6	1.070	1.070	1.070	1.070	1.070	1.070
7	1.064	1.063	1.061	1.060	1.058	1.057
8	1.090	1.090	1.090	1.090	1.090	1.090
9	1.057	1.055	1.053	1.051	1.049	1.046
10	1.053	1.050	1.0488	1.045	1.043	1.040
11	1.058	1.056	1.055	1.053	1.021	1.050
12	1.057	1.055	1.054	1.052	1.050	1.049
13	1.052	1.050	1.048	1.046	1.044	1.041
14	1.039	1.035	1.031	1.027	1.023	1.018

Table 5. Variation in active power flow with change in transmission parameter IEEE-14 Bus system

Line No.	Active Power Flow (MW)					
	-10%	Base Case	10%	20%	30%	40%
1	85.878	86.620	86.242	87.018	87.432	87.861
2	48.049	48.415	48.241	48.586	48.754	48.920
3	40.363	40.679	40.494	40.856	41.026	41.192
4	41.348	41.431	41.401	41.473	41.524	41.584
5	31.321	31.386	31.363	31.420	31.462	31.511
6	-4.515	-4.340	-4.456	-4.235	-4.139	-4.049
7	-42.79	-42.67	-42.74	-42.59	-42.52	-42.45
8	18.437	18.418	18.424	18.413	18.409	18.405
9	12.536	12.511	12.521	12.502	12.492	12.483
10	27.264	27.437	27.356	27.517	27.598	27.697
11	9.321	9.382	9.355	9.409	9.436	9.463
12	8.012	8.046	8.030	8.063	8.079	8.095
13	18.731	18.809	18.772	18.846	18.883	18.921
14	-10.00	-10.00	-10.00	-10.00	-10.00	-10.00
15	28.437	28.418	28.424	28.413	28.409	28.405
16	3.281	3.246	3.260	3.232	3.218	3.205
17	8.191	8.183	8.184	8.183	8.183	8.183
18	-5.728	-5.765	-5.49	-5.780	-5.794	-5.808
19	1.844	1.863	1.855	1.871	1.879	1.887
20	6.863	6.907	6.888	6.926	6.945	6.963

3.3. Case-3

The shunt controller is placed at the bus, which has low voltage after performing maximum load variation and does not have any nearby generator support.

Therefore, bus-4 is considered an optimal location for this system to install SVC. Then Q_{sh} is varied from -100 to +100 in step 40 at bus-4 to analyze its effect.

Table 6. variation in apparent power flow with change in transmission parameter IEEE-14 Bus system

Line No.	Apparent Power Flow (MVA)						Line limit
	-10%	Base Case	10%	20%	30%	40%	
1	85.880	86.274	86.746	87.266	87.813	88.375	150
2	48.323	48.432	48.547	48.681	48.826	48.978	85
3	41.296	41.245	41.163	41.164	41.219	41.310	85
4	41.361	41.417	41.454	41.501	41.556	41.616	85
5	31.330	31.367	31.387	31.420	31.462	31.512	85
6	9.623	8.796	7.509	6.467	5.626	4.958	85
7	43.495	43.387	43.325	43.268	43.214	43.162	150
8	20.433	20.099	19.808	19.583	19.406	19.264	30
9	12.543	12.531	12.526	12.522	12.518	12.515	32
10	31.652	30.691	30.044	29.576	29.235	28.988	45
11	9.729	9.810	9.872	9.933	9.992	10.052	14
12	8.349	8.377	8.402	8.427	8.452	8.477	32
13	19.926	20.009	20.082	20.154	20.226	20.298	22
14	20.013	19.290	18.643	18.130	17.718	17.385	2
15	29.490	29.445	29.421	29.403	29.392	29.386	29
16	6.011	5.884	5.802	5.726	5.655	5.588	32
17	9.174	9.137	9.120	9.106	9.094	9.083	18
18	5.752	5.824	5.854	5.884	5.913	5.942	12
19	1.942	1.959	1.972	1.984	1.997	2.009	12
20	6.965	7.008	7.041	7.074	7.106	7.139	12

The variations in voltage magnitude with the installation of SVC are shown in Table.7. From the table; it is visible that the voltage magnitude is increasing with an increase in Q_{sh} .

The variations in active power flow with the installation of SVC are shown in Table. 8. The variations in apparent power flow with the installation of SVC are shown in the table.9.

Table 7. Variation in voltage magnitude with the installation of SVC for IEEE-14 Bus system

Line No.	Voltage Magnitude (p.u)						
	-100	-60	-20	Base Case	20	60	100
1	1.06	1.06	1.06	1.06	1.06	1.06	1.06
2	1.040	1.045	1.045	1.045	1.045	1.045	1.045
3	1.01	1.01	1.01	1.01	1.012	1.022	1.032
4	0.975	0.998	1.0141	1.021	1.031	1.049	1.067
5	0.998	1.010	1.020	1.024	1.030	1.041	1.054
6	1.059	1.07	1.07	1.07	1.07	1.07	1.079
7	1.032	1.051	1.058	1.061	1.066	1.074	1.084
8	1.071	1.09	1.09	1.09	1.09	1.09	1.09
9	1.026	1.044	1.051	1.052	1.058	1.065	1.076
10	1.024	1.041	1.047	1.047	1.053	1.059	1.070
11	1.038	1.052	1.054	1.055	1.057	1.060	1.071
12	1.043	1.054	1.054	1.054	1.055	1.056	1.065
13	1.037	1.048	1.049	1.048	1.050	1.051	1.061
14	1.012	1.028	1.032	1.032	1.037	1.041	1.052

Table 8. Variation of active power flow with the installation of SVC for IEEE-14 Bus system

Line No.	Active power flow (MW)						
	-100	-60	-20	Base Case	20	60	100
1	88.353	87.149	86.476	95.934	86.059	85.861	85.792
2	47.451	47.702	48.034	52.423	48.453	48.922	49.604
3	42.317	41.339	40.755	44.181	40.348	40.260	40.181
4	41.306	41.291	41.337	44.086	41.433	41.480	41.552
5	31.670	31.507	31.393	33.293	31.300	31.148	31.087
6	-2.684	-3.639	-4.203	-5.608	-4.585	-4.643	-4.713
7	-41.06	-41.80	-42.42	-45.84	-43.02	-43.51	-43.72
8	18.080	18.230	18.359	19.773	18.496	18.656	18.536
9	12.235	12.337	12.460	13.288	12.587	12.732	12.721
10	28.085	27.772	27.490	29.688	27.209	26.903	27.030
11	9.679	9.541	9.414	9.781	9.288	9.149	9.240
12	8.186	8.119	8.059	8.440	7.998	7.934	7.933
13	19.020	18.912	18.817	19.706	18.722	18.619	18.656
14	-10	-10	-10	-10	-10	-10	-10
15	28.080	28.230	29.773	29.773	28.496	28.656	28.536
16	2.986	3.095	3.471	3.471	3.323	3.462	3.373
17	7.828	7.972	8.615	8.615	8.261	8.427	8.383
18	-6.016	-5.909	-5.989	-5.989	-5.689	-5.556	-5.645
19	2.003	1.940	1.952	1.952	1.824	1.761	1.763
20	7.253	7.099	7.218	7.218	6.812	6.655	6.698

Table 9. Variation apparent power flow with the installation of SVC for IEEE-14 Bus system

Line No.	Apparent Power Flow (MVA)							Line Limit
	100	60	20	Base Case	20	60	100	
1	88.52	87.188	86.511	96.066	86.090	85.890	85.821	150
2	51.084	49.055	48.493	52.594	48.487	49.063	50.477	85
3	42.614	42.049	41.493	44.771	40.858	40.284	40.380	85
4	47.531	43.336	41.489	44.100	41.882	44.608	49.765	85
5	35.444	32.890	31.581	33.299	31.408	32.426	35.186	85
6	19.976	7.559	5.122	8.501	11.932	16.563	21.725	85
7	51.271	44.456	42.423	46.568	45.747	54.458	65.699	150
8	24.321	23.456	21.038	21.310	19.328	18.662	19.060	30
9	12.659	12.550	12.467	13.306	12.677	13.244	13.806	32
10	28.345	28.586	29.818	32.620	31.795	34.652	36.027	45
11	11.809	10.851	10.108	10.364	9.541	9.168	9.242	14
12	8.677	8.546	8.431	8.819	8.319	8.203	8.189	32
13	21.003	20.563	20.184	21.073	19.828	19.473	19.452	22
14	25.045	24.921	21.104	19.959	17.414	13.840	10.617	32
15	28.604	29.076	29.321	30.951	29.583	29.884	29.473	29
16	3.216	4.124	5.268	5.948	6.566	80.045	8.345	32
17	8.008	8.406	8.887	9.531	9.433	10.108	10.204	18
18	7.582	6.667	6.029	6.125	5.691	5.733	5.920	12
19	2.288	2.142	2.015	2.075	1.900	1.793	1.785	12
20	8.139	7.592	7.173	7.386	6.860	6.658	6.712	12

Table 10. Variation in voltage magnitude with the installation of TCSC for IEEE-14 Bus system

Bus No.	Voltage Magnitude(p.u)					
	+20%	Base Case	-20%	-40%	-60%	-80%
1	1.065	1.060	1.060	1.060	1.060	1.060
2	1.045	1.045	1.045	1.045	1.045	1.045
3	1.010	1.010	1.010	1.010	1.010	1.010
4	1.023	1.022	1.023	1.022	1.022	1.022
5	1.025	1.024	1.026	1.026	1.026	1.027
6	1.070	1.070	1.070	1.070	1.070	1.070
7	1.063	1.061	1.062	1.062	1.062	1.062
8	1.090	1.090	1.090	1.090	1.090	1.090
9	1.055	1.053	1.055	1.055	1.055	1.055
10	1.050	1.048	1.050	1.050	1.050	1.050
11	1.056	1.055	1.056	1.056	1.056	1.056
12	1.055	1.054	1.055	1.055	1.055	1.055
13	1.050	1.049	1.050	1050	1.050	1.050
14	1.035	1.032	1.035	1.035	1.035	1.035

After the installation of SVC, during the absorption of reactive power, the active power loss increases as the shunt reactance increases. During the injection of reactive power, the active power loss increases with the decrease in shunt reactance.

Table 11. Variation in voltage magnitude with the installation of TCSC for IEEE-14 Bus system

Line No.	Active Power Flow (MW)					
	+20%	Base Case	-20%	-40%	-60%	-80%
1	86.698	95.934	85.758	85.244	84.697	84.117
2	47.796	52.423	48.717	49.226	49.772	50.357
3	40.846	44.181	40.122	39.727	39.307	38.863
4	42.158	44.087	40.596	39.738	38.825	37.582
5	30.697	33.293	32.071	32.825	33.627	34.482
6	-4.117	-5.609	-4.816	-5.199	-5.604	-6.035
7	-41.31	-45.843	-44.27	-45.90	-47.64	-49.49
8	18.187	19.773	18.677	18.947	19.236	19.546
9	12.385	13.288	12.665	12.820	12.984	13.161
10	27.737	29.688	26.950	26.517	26.053	25.558
11	9.588	9.781	9.106	8.840	8.555	8.251
12	8.058	8.441	8.000	7.968	7.934	7.898
13	18.891	19.706	18.645	18.509	18.364	18.209
14	-10.00	-10.000	-10.00	-10.00	-10.00	-10.00
15	28.187	29.773	28.677	28.947	29.236	29.546
16	3.032	3.471	3.504	3.765	4.044	4.343
17	8.040	8.616	8.337	8.501	8.677	8.864
18	-5.978	-5.989	-5.506	-5.245	-4.966	-4.668
19	1.883	1.952	1.825	1.794	1.760	1.724
20	7.032	7.218	6.773	6.569	6.393	6.205

Table 12. Variation of apparent power flow with installation of TCSC for IEEE-14 bus system

Line No.	Apparent Power Flow (MVA)						Line Limit
	+20%	Base Case	-20%	-40%	-60%	-80%	
1	86.733	96.066	85.787	85.269	84.720	84.136	150
2	48.007	52.595	48.887	49.373	49.894	50.454	85
3	41.579	44.771	40.891	40.516	40.119	39.698	85
4	42.193	44.100	40.604	39.741	38.825	37.855	85
5	30.709	33.300	32.701	32.827	33.638	34.512	85
6	8.830	8.501	8.762	8.732	8.705	8.686	85
7	41.852	46.568	45.035	46.811	48.728	50.804	150
8	19.855	21.311	20.363	20.649	20.961	21.302	30
9	12.397	13.307	12.673	12.826	12.989	13.164	32
10	30.979	32.620	30.395	30.093	29.790	29.489	45
11	10.011	10.365	9.600	9.379	9.150	8.911	14
12	8.400	8.820	8.353	8.327	8.300	8.272	32
13	20.109	21.074	19.904	19.794	19.677	19.554	22
14	19.285	19.960	19.304	19.327	19.364	19.416	32
15	29.238	30.951	29.668	29.906	30.161	30.436	29
16	5.835	5.949	5.944	6.018	6.107	6.214	32
17	9.034	9.531	9.247	9.365	9.492	9.629	18
18	6.037	6.126	5.600	5.366	5.122	4.869	12
19	1.980	2.075	1.936	1.913	1.889	1.864	12
20	7.140	7.387	6.869	6.722	6.568	6.407	12

Table 13. Variation in active power loss in different cases for IEEE-14 bus system

P Loss at Wide Load Variations in active power loss in different cases for IEEE-14 bus system						
Base Case	1% Load	2% Load	3% Load	4 % Load	5% Load	
5.482537	5.660321	5.841722	6.02675	6.215418	6.407735	
P Loss with different transmission parameters variations for IEEE-14 bus system						
-10%	Base case	10%	20%	30%	40%	
4.927315	5.482537	6.035579	6.603895	7.186023	7.781031	
P Loss with the installation of SVC for IEEE-14 bus system						
-100	-60	-20	Base Case	20	60	100
6.804608	5.851962	5.51188	6.407735	5.513309	5.78338	6.396781
P Loss with the installation of TCSC for IEEE-14 bus system						
20%	Base Case	-20%	-40%	-60%	-80%	
5.493202	6.407735	5.474487	5.469799	5.469422	5.474564	

3.4. Case-4

In case 4, the basic variable impedance series (Thyristor controlled series compensator—TCSC) controller is taken into consideration by confirming the maximum load fluctuation of the system in order to analyze the impact of FACTS controllers on the system performance.

The series controller is placed in a line which is having high power flow margin (i.e., the difference between line limit

and actual power flow). For this system, line-7, i.e., connected between buses 5 and 4, is considered the optimal location. Then the reactance in that line, i.e., line-7, is varied from -20% to +20% in steps of 20% to analyze its effect. The variations in voltage magnitude with the installation of TCSC are shown in Table.10. By observing this table; it is said that the voltage magnitude increases with an increase in reactance value. The variations in active power flow with the installation of TCSC are shown in Table.11. The variations in apparent power flow

with the installation of TCSC along with the line limits are shown in Table.12. The variations in active power loss in different cases for IEEE-14 bus system as shown in Table.13.

Because of the increased load, the active power loss in the power system increases. When the load increases, current consumption in the system increases, and hence I^2R losses also increase. The active power losses also increase due to an increase in transmission parameters R and X and decrease due to the installation of TCSC.

4. Conclusion

The power system performance is better at the load centers when compared to the normal type of power system performance without an analytical process. The consumer can

meet the required load, and the generating station can maintain maximum power flow limits. A complete mathematical formulation to resolve The issue with load flow has been presented with a supporting load flow incorporation procedure. From the pre-analysis, it has been notified that the power system's total performance has been enhanced in terms of voltage profile, decreased total losses, etc. The analysis is very useful in the aspects of planning for the new system, connecting a new load, economical scheduling, controlling, installing new equipment and operating the system at its maximum limits. Finally, the effect of FACTs controllers on power system performance in terms of voltage, power flow, power losses, generation cost, emission etc, have been analyzed. From this survey, it has been observed that there has been notable enhancement of system performance in the existence of FACTs controllers on the power systems.

References

- [1] Xi-Fan Wang, Yonghua Song, and Malcolm Irving, *Modern Power Systems Analysis*, Springer, 2009. [[Google Scholar](#)] [[Publisher Link](#)]
- [2] John J. Grainger, and William D. Stevenson, *Power System Analysis*, Mcgraw-Hill: ISBN 0-07-061293-5, 1994. [[Google Scholar](#)] [[Publisher Link](#)]
- [3] Glenn W. Stagg, and Ahmed H. El-Abiad, *Computer Methods in Power Systems*, Mcgraw-Hill, 1968.
- [4] H.E. Brown et al., "Power Flow Solution by Impedance Matrix Iterative Method," *IEEE Transactions on Power Apparatus and System*, vol. 82, no. 65, pp. 1-10, 1963. [[CrossRef](#)] [[Google Scholar](#)] [[Publisher Link](#)]
- [5] Annapoorani Anantharaman, "A Study of Logistic Regression And Its Optimization Techniques Using Octave," *SSRG International Journal of Computer Science and Engineering*, vol. 6, no. 10, pp. 23-28, 2019. [[CrossRef](#)] [[Google Scholar](#)] [[Publisher Link](#)]
- [6] William F. Tinney, and Clifford E. Hart, "Power Flow Solution by Newton's Method," *IEEE Transactions on Power Apparatus and Systems*, vol. PAS-86, no. 11, pp. 1449-1460, 1967. [[CrossRef](#)] [[Google Scholar](#)] [[Publisher Link](#)]
- [7] B. Stott, and O. Alasc, "Fast Decoupled Load Flow," *IEEE Transactions on Power Apparatus and Systems*, vol. PAS-93, no. 3, pp. 859-869, 1974. [[CrossRef](#)] [[Google Scholar](#)] [[Publisher Link](#)]
- [8] Allen J. Wood, and F. Bruce, *Power Generation, Operation, and Control*, John Wiley & Sons, 1996. [[Google Scholar](#)]
- [9] P.S.R. Murty, *Operation and Control in Power Systems*, BS Publications, 2011. [Online]. Available: https://www.bspublications.net/book_detail.php?bid=887
- [10] Dhanush Patel et al., "Voltage Stability Improvement using Thyristor Controlled Series Capacitor," *SSRG International Journal of Electrical and Electronics Engineering*, vol. 3, no. 5, pp. 1-3, 2016. [[CrossRef](#)] [[Publisher Link](#)]
- [11] W.L. Chan, A.T.P. So, and L.L. La, "Initial Applications of Complex Artificial Neural Networks to Load-Flow Analysis," *IEEE Proceedings of Generation Transmission Distribution*, vol. 147, no. 6, pp. 361-366, 2000. [[CrossRef](#)] [[Google Scholar](#)] [[Publisher Link](#)]
- [12] K.P. Wong, A. Li, and T.M.Y. Law, "Advanced Constrained Genetic Algorithm Load Flow Method," *IEEE Proceedings Of Generation Transmission Distribution*, vol. 146, no.6, pp. 609-616, 1999. [[CrossRef](#)] [[Google Scholar](#)] [[Publisher Link](#)]
- [13] K.L. Lo, Y.J. Lin, and W.H. Siew, "Fuzzy-Logic Method for Adjustment of Variable Parameters in Load Flow Calculation," *IEEE Proceedings of Generation Transmission Distribution*, vol. 146, no. 3, pp. 276-282, 1999. [[CrossRef](#)] [[Google Scholar](#)] [[Publisher Link](#)]
- [14] M.A. Pai, *Computer Techniques in Power System Analysis*, Tata McGraw-Hill Publishing Company Ltd, India, pp. 228-228, 2006.
- [15] Pulakesh Kumar Kalita, and Satyajit Bhuyan, "Study of FACTS Controllers and Its Impact on Power Quality," *SSRG International Journal of Electrical and Electronics Engineering*, vol. 5, no. 6, pp. 34-40, 2018. [[CrossRef](#)] [[Publisher Link](#)]
- [16] Abdulhalim Musa Abubakar, and Ahmad Abubakar Mustapha, "Newton's Method Cubic Equation of State C++ Source Code for Iterative Volume Computation," *International Journal of Recent Engineering Science*, vol. 8, no. 3, pp. 12-22, 2021. [[CrossRef](#)] [[Google Scholar](#)] [[Publisher Link](#)]
- [17] Robert G. Andretich et al., "The Piecewise Solution of The Impedance Matrix Load Flow," *IEEE Transactions on Power Apparatus and Systems*, vol. PAS-87, no. 10, pp.1877-1882, 1968. [[CrossRef](#)] [[Google Scholar](#)] [[Publisher Link](#)]
- [18] K. Niteesh Kumar, and Ch. Chengaiah, "Reducing Generation Cost in Transmission System using FACTS Devices," *SSRG International Journal of Electrical and Electronics Engineering*, vol. 2, no. 11, pp. 12-16, 2015. [[CrossRef](#)] [[Publisher Link](#)]
- [19] T.T. Nguyen, "Neural Network Load-Flow," *IEEE Proceedings of Generation Transmission Distribution*, vol. 142, no. 1, pp. 51-58, 1995. [[CrossRef](#)] [[Google Scholar](#)] [[Publisher Link](#)]